

Influence of the Fermi velocity on the transport properties of the 3D topological insulators

A.M. Korol^{1,2} and N.V. Medvid²

¹Laboratory on Quantum Theory in Linköping, ISIR, P.O. Box 8017, S-580, Linköping, Sweden
E-mail: korolam@ukr.net

²National University for Food Technologies, 68 Volodymyrska str., Kyiv, Ukraine

Received January 9, 2019, revised March 26, 2019, published online August 27, 2019

We explore the transport of the surface states quasielectrons in the 3D topological insulators through the barriers of various origin: the Fermi velocity and the electrostatic barriers. These barriers are believed to be the rectangular and one-dimensional ones. The transmission coefficient T as the function of the quasiparticle energy E and an angle of incidence θ (transmission spectra) is evaluated with the help of the effective Hamiltonian; the conductivity G is calculated on the base of the Landauer–Buttiker formula. It is shown that the value of T and G significantly depends on the ratio of the Fermi velocities in the barrier and out-of-barrier regions $\alpha = v_{F2}/v_{F1}$. The dependence of these quantities on the strength of the electrostatic potential is analyzed. We find in particular that the effect of supertunneling manifests itself in the considered structure — being markedly dependent on the value of α . The formula which points out the energy value for which the effect of supertunneling takes place, for different α , is presented. For normal angle of the particle incidence, there is the effect analogous to the Klein paradox. The spectra $T(E, \theta)$ and $G(E)$ substantially depend on the interplay of α , energy E and the magnitude of the electrostatic potential. Hence, by changing the problem parameters one can flexibly vary the spectra of $T(E, \theta)$ and $G(E)$ in wide limits. The obtained results may be useful for the nanoelectronics based on the topological insulators.

Keywords: topological insulators, potential barriers, Fermi velocity, transmission spectra.

1. Introduction

Topological insulators belong to the new class of substances that have recently been called Dirac materials ([1] and references therein). These include very different objects in their structure, in particular the low- and high-temperature d -wave superconductors, superfluid phases ³He, graphene, two- and three-dimensional insulators etc. [1].

The key concept that unites these different objects is a linear dispersion relation that describes the low-energy excitations of the quasiparticles. Due to the fact that the Dirac materials have a number of non-trivial, interesting properties, they — and topological insulators (TI) among them — are actively studied in the last time (e.g., [2–13]). The most important characteristic of TI is that they are insulators in their volume, but are capable of conducting the electric current on their surface. These surface states can contribute to charge transport at low energies. Under low energies, the surface states of TI are described by a massless Dirac equation in one or two dimensions, analo-

gous to the equation for the quasielectrons in graphene. The dispersion relation for the Dirac particles relates to a cone in the three-dimensional case. Some properties of surface states of TI are expressed in terms of topologically invariant quantities and, importantly, are protected from the influence of moderate perturbations due to the symmetry of inversion of time in the corresponding Hamiltonian. Time reversal invariant perturbations such as lattice imperfections or non-magnetic moderate disorder do not produce a gap; at the same time the external magnetic field can produce a gap for the surface states.

Quasielectrons in TI exhibit strong spin-orbital interaction. Due to this and due to the time-reversal symmetry, the surface states of TIs have an odd number of Dirac cones and expose the chiral spin nature (as observed by the angle-resolved photo-emission spectroscopy). Directions of the linear and the spin-angular quasi-momenta of quasielectrons on the surface of TI are interconnected and perpendicular to each other. Also we should keep in mind that the surface Hamiltonian of the 3D TI deals with the real

spin (in contrast with the graphene where the respective Hamiltonian comprises the pseudospin term).

There are two classes of topological insulators: two (2D) and three-dimensional (3D) TI. The first ones are also called quantum spin Hall dielectrics, and they can be realized in quantum wells of HgCdTe compounds. Three-dimensional TIs are represented by bismuth compounds Bi₂Se₃, Bi₂Te₃ and similar materials. There are also strong and weak 3D TIs. Surface states in 2D and 3D TIs are one-dimensional and two-dimensional, respectively.

It is known that the Dirac excitations in TI exhibit the Klein tunneling (as in graphene) for normal incidence of the quasielectrons on the barrier.

It is convenient to control the behavior of fermions in Dirac materials by means of external electric and magnetic fields, and a lot of publications are devoted to the corresponding problem for this reason.

At the same time, since the Fermi velocity fully characterizes the Dirac cone slopes, i.e., the linear dispersion relation, it is essential for applications. Therefore recently one more way for controlling the electronic properties of the Dirac materials namely by means of the spatial change of the Fermi velocity (in particular with the help of doping) was offered (e.g., [17–20] and references therein). A lot of propositions to use this control in practice were also published [14–21].

2D and 3D TI may be useful in practice in particular in quantum computation and spintronics.

Motivated by the above mentioned statements we analyze here the transmission of the Dirac quasiparticles through the velocity and electrostatic barriers in the 3D topological insulators.

2. Model and formulae

Consider the motion of the quasielectrons of the topological insulator surface states along the Ox axis from the left to the right. Assume that there is the rectangular one-dimensional electrostatic potential barrier with the height U and width D , the interfaces coordinates being $x_l = 0$ and $x_r = D$ for the left and the right interface, respectively.

The low-energy excitations of the surface states in TI can be described by the following Hamiltonian [4,10]:

$$H = -i\hbar v_F \left(\sigma_y \frac{\partial}{\partial x} - \sigma_x \frac{\partial}{\partial y} \right) + \sigma_0 U, \quad (1)$$

where v_F is the Fermi velocity, σ_x , σ_y are the Pauli matrices and σ_0 the unit matrix.

In the case when the Fermi velocity varies in space this Hamiltonian is not the Hermitian one [4,10]. Assume that the Fermi velocity depends on the coordinate x (only) and let $\hbar = 1$. As usual in the relevant cases, it is assumed also that the barrier width is much larger than the near-interface regions associated with the gradual change in the Fermi velocity. Then in accordance with the considerations made

in [4,10] we may present the Hamiltonian of the problem as follows:

$$H = -i\sqrt{v_F(x)} \left[\sigma_y \frac{\partial}{\partial x} \sqrt{v_F(x)} - \sigma_x \frac{\partial}{\partial y} \right] + \sigma_0 U, \quad (2)$$

and now it has the hermitian form [4,10]. We must keep in mind that the derivative acts on the product $\sqrt{v_F(x)}\psi = \phi$ where ψ are the spinorial eigenfunctions. The conservation of the local current requires the function ϕ to be continuous at the interfaces [4,10], that is

$$\begin{aligned} \sqrt{v_{F1}}\psi_l(x=0^-) &= \sqrt{v_{F2}}\psi_b(x=0^+), \\ \sqrt{v_{F2}}\psi_b(x=D^-) &= \sqrt{v_{F1}}\psi_r(x=D^+), \end{aligned} \quad (3)$$

where $\psi_{l,r}$ and ψ_b are the eigenfunctions in the left (l) and right (r) out-of-barrier and in the barrier (b) regions, respectively, v_{F1} , v_{F2} are the Fermi velocities in the barrier and out-of-barrier regions, respectively.

If the electron wave moves along the axis Ox from the left to the right, then for the wave functions in the left and the right out-of-barrier regions it is possible to write, respectively:

$$\begin{aligned} \psi_l(x) &= \frac{1}{\sqrt{2}} \begin{pmatrix} 1 \\ f^- \end{pmatrix} e^{ik_x x} + \frac{r}{\sqrt{2}} \begin{pmatrix} 1 \\ f^+ \end{pmatrix} e^{-ik_x x}, \\ \psi_r(x) &= \frac{t}{\sqrt{2}} \begin{pmatrix} 1 \\ f^- \end{pmatrix} e^{ik_x x}, \end{aligned} \quad (4)$$

where $f^\mp \equiv (\mp k_x + k_y) / E$;
for the barrier area we have

$$\begin{aligned} \psi_b(x) &= \frac{a}{\sqrt{2}} \begin{pmatrix} 1 \\ g^+ \end{pmatrix} e^{iq_x x} + \frac{b}{\sqrt{2}} \begin{pmatrix} 1 \\ g^- \end{pmatrix} e^{-iq_x x}, \\ g^\mp &= \frac{\mp iq_x + k_y}{(E-U)\alpha^{-1}}, \end{aligned} \quad (5)$$

$$k_x = \sqrt{E^2 - k_y^2}; \quad q_x = \sqrt{\frac{(E-U)^2}{\alpha^2} - k_y^2}; \quad (6)$$

$$\begin{aligned} k_x &= E \cos \theta, \quad k_y = E \sin \theta, \quad \varphi = \arctan(k_y / q_x), \\ \alpha &= v_{F2} / v_{F1}. \end{aligned} \quad (7)$$

Using the boundary conditions (3) we find the coefficients in expressions for the wave functions, and hence the transmission coefficient $T = |t|^2$:

$$\begin{aligned} T(E, \theta) &= \left\{ (\cos(q_x D))^2 + (\sin(q_x D))^2 \times \right. \\ &\times \left. \left[(\cos \theta)^{-1} (\sin \varphi)^{-1} + \text{sign}(E-U) \tan \theta \tan \varphi \right]^2 \right\}^{-1}. \end{aligned} \quad (8)$$

3. Results and discussion

From the above formulas, it is clear that the difference in the values of the Fermi velocity in the barrier and the out-of-barrier regions has a definite influence on the transmission spectra of the considered structure. The question is how essential this effect can be.

Consider the case of the presence of the combined Fermi velocity barriers and the electrostatic barriers. Figure 1 depicts the dependence of the transmission coefficient T on an angle of the quasielectrons incidence onto the structure θ for their fixed energy $E = 1.5$ for several values of α , namely, the curves $T1, T2, T3$ correspond to values of $\alpha = 0.5; 1; 2$; other parameters are $U = 3, D = 3$. It is seen that the change in the Fermi velocity in the barrier region makes a strong influence on the transmission spectra. The non-trivial feature of the given spectra is the manifestation of the phenomenon of supertunneling, which consists in the fact that for electron energy value equal to half the height of the potential barrier $E = U/2$, the transmission through the barrier region is perfect for any angle of incidence (see line 2 in Fig. 1).

We emphasize that for the Fermi velocity values in a barrier with $\alpha \neq 1$, the phenomenon of supertunneling also occurs, but for energies other than $E = U/2$. As shown below, for the case $\alpha \neq 1$, there are certain energies for which the transmission is ideal for any angle of incidence.

Figure 1 shows also that in the considered structure, in addition to the effect of supertunneling, a phenomenon similar to the Klein tunneling is observed: the barrier transparency is perfect for particles that fall to the barrier normally. Klein tunneling takes place for any values of α , that is, the Fermi velocity barriers are absolutely transparent in the case of normal incidence of particles for any height of the velocity barriers and of the electrostatic barriers.

The value of the transmission rates T for a fixed angle of incidence θ is an oscillating value, depending on the magnitude of α . The region of the angles of incidence θ for which $T(\theta)$ is high can be broad, see curve $T1$ in Fig. 1 for which $\alpha = 0.5$. Although the general trend is such that, with increasing an angle of incidence the coefficient T de-

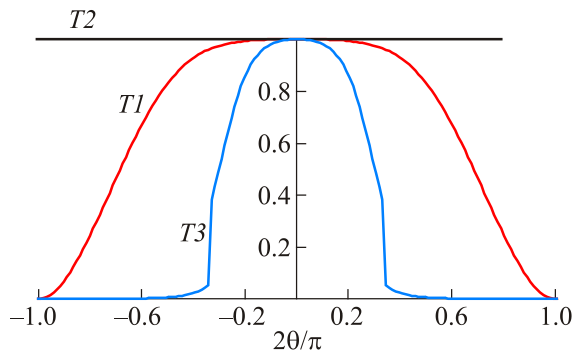


Fig. 1. (Color online) Dependence of the transmission rates T on an angle of incidence for the parameters: $E = 1.5, U = 3, D = 3, \alpha = 0.5; 1; 2$, respectively, for the curves $T1, T2, T3$.

creases on average, but for certain values of α , the value of T can be significant even for large angles of incidence.

Figure 2 shows the dependence $T(\theta)$ for the energy close to the electrostatic barrier height for three different values of $\alpha = 0.5; 1; 2$ for curves $T1, T2, T3$, respectively. It is seen that the number of resonance peaks increases with decreasing α (for the case $E \ll U$, the dependence $T(\theta)$ is described by a smooth line throughout the range of values of angles $-\pi/2 < \theta < \pi/2$ (see Fig. 1)). For $\alpha > 1$, there is only a narrow range of values of angles θ — in the vicinity of $\theta = 0$ — in which $T(\theta) \neq 0$ and can reach large values. This is explained by the fact that for energies $E \sim U$ for most angles θ , the quasi-momentum q becomes imaginary and the electron wave becomes evanescent (see formulae (6)). The spectra for the case of large energies (in comparison with the height of the barrier) are characterized by the presence of many resonance peaks which correspond to the condition for formation of the resonance states of the Fabry–Perot type:

$$D\sqrt{\frac{(E-U)^2}{\alpha^2} - k_y^2} = n\pi. \quad (9)$$

These maxima are related to the so-called “magic angles”. It is obvious from the condition (9) that more resonances are formed at higher energies. The studied transmission spectra are characterized by the presence of a critical angle of the quasiparticles incidence on the structure θ_c . For angles of incidence θ greater than θ_c , the quasiparticles cannot penetrate through the barrier (see, in particular, the spectra in Figs. 1 and 2). The value of the critical angle can be found from the Snell law and it is equal to

$$\theta_c = \pm \arcsin\left(\frac{|E-U|}{\alpha E}\right). \quad (10)$$

Depending on the particles energy E and on the height of the potential barrier height U the critical angle may be formed for both cases of $\alpha > 1$ and $\alpha < 1$. The values of

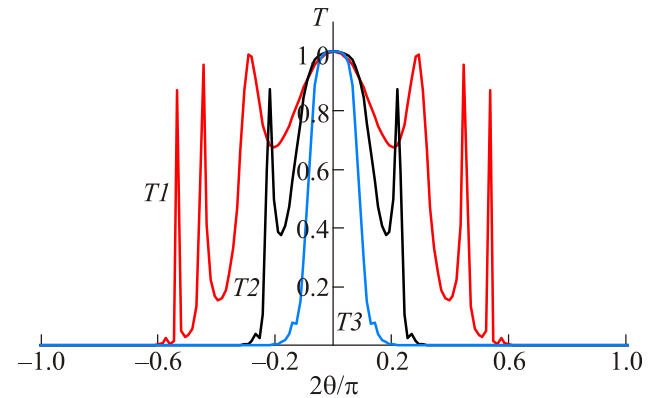


Fig. 2. (Color online) T vs θ plot with the parameters: $E = 4, U = 3, D = 3, \alpha = 0.5; 1; 2$, respectively, for the curves $T1, T2, T3$.

$\alpha > 1$ are associated with the barriers for electrons and in this case the range of values of E and U for which there is a critical angle is rather broad — unlike for the case $\alpha < 1$ (which is associated with the quantum wells).

The range of angles of incidence θ for which the value of $T(\theta)$ is significant as well as the values of the critical angle θ_c , are substantially reduced with increasing in α . Figure 3 shows the dependence of the coefficient T on energy E for a fixed angle of incidence $\theta = \pi/4$ and values of $\alpha = 0.5; 1; 2$ for the curves 1, 2, 3, respectively, and others the parameters are $U = 3, D = 3$.

It is clearly seen that there exist the resonant values of energy E_r for which the transparency of the structure is perfect, that is $T(E_r) = 1$. For each value of α , there is such an energy for which the phenomenon of supertunneling is realized; we can deduce the expression for this energy from the above formulae and it reads

$$E_s = \frac{U}{1 + \alpha}. \tag{11}$$

Consequently, the energy position associated with the phenomenon of supertunneling depends essentially on the ratio of the Fermi velocities in the barrier and in the out-of-barrier regions. The value of E_s decreases with increasing of α regardless of whether we are dealing with the barriers ($\alpha > 1$) or with the quantum wells ($\alpha < 1$).

Now we can state that the spectra $T(E)$ have the following structure in general:

1. The presence of peaks in the dependence of $T(E)$ (and also in the dependence of $T(\theta)$) indicates that the transmission of quasielectrons in the structure considered has a resonant-tunneling character.
2. For energy $E_s = U / (1 + \alpha)$, the transmission coefficient $T = 1$ for all θ (the effect of supertunneling).
3. There is a plateau of energies with values of $T \sim 1$ in the vicinity of the point E_s .

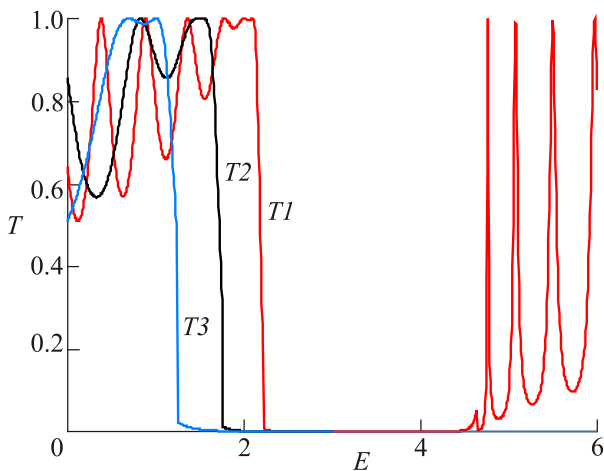


Fig. 3. (Color online) T vs E plot for the following parameters: $\theta = \pi/4, U = 3, D = 3, \alpha = 0.5; 1; 2$, respectively, for the curves $T1, T2, T3$.

4. There is a wide gap in the vicinity of energy $E \sim U$. Its width sharply depends on an angle of incidence θ increasing with increasing of θ .

5. There are Fabry–Perot-like resonances with values $T = 1$ in the regions distant from the point E_s under the condition $E < U, E_s$. If conditions for the formation of a critical angle are not fulfilled, similar resonances exist for energies $E > U, E_s$. The Fabry–Perot-type resonances are placed on the axis of energy periodically.

6. If there is a critical angle then T decreases sharply with E increasing. The steepness of the function $T(E)$ depends on the parameters of the problem. The critical energy E_c corresponds to the critical angle θ_c : for the electrons with energy $E > E_c$ the barrier is insurmountable. According to formula (9), the critical energy is equal to

$$E_c = \frac{U}{|\alpha \sin \theta_c - 1|}. \tag{12}$$

In Figure 4, the dimensionless conductivity G (the quantity that can be measured in experiment) is presented as the function of energy E . It takes into account the combined Fermi velocity barriers and the electrostatic barriers. The values of the parameters for this figure are as follows: $D = 1, U = 2$, lines 1, 2, 3 correspond to values of $\alpha = 0.5; 1; 2$, respectively.

First of all, it is noteworthy that the function $G(E)$ has an oscillating character, which corresponds to the dependences of the transmission coefficient T on energy E . At the points $E_s = U / (1 + \alpha)$, the maximum values of conductivity due to the effect of supertunneling are realized and the given condition of maxima is performed precisely. In the energy region $E \sim U$, there is a fairly wide range of energies in which the function $G(E)$ has a minimal value — this region is associated with the gap in the $T(E)$ dependences. Its width increases markedly with an increase of α (compare curves 1, 2, 3). On average, the growth of α leads to a decrease in conductivity.

At energies somewhat smaller and larger than those corresponding to the minimum $G(E)$, oscillations of con-

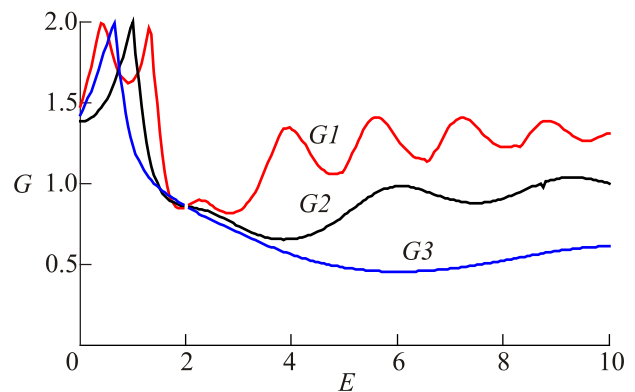


Fig. 4. (Color online) Dependences of the dimensionless conductivity G on energy E for the following parameters: $D = 1; U = 2; \alpha = 0.5; 1; 2$ for $G1, G2, G3$, respectively.

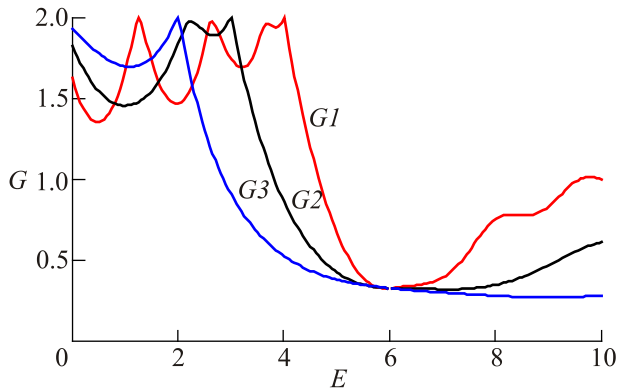


Fig. 5. (Color online) Dependences of the dimensionless conductivity on energy E for the following parameters: $D = 1$; $U = 6$; $\alpha = 0.5$; 1; 2 for $G1$, $G2$, $G3$, respectively.

ductivity are observed. In the region of smaller energies, the value of $G(E)$ reaches a maximum, and in the right side of the spectra the value of G is much smaller. These oscillations are related to Fabry–Perot resonances in the dependences $T(E)$. The difference in the regions of smaller and larger energies is explained in this way: in the region of energies $E \cong 0.5U$, the half-widths of the resonances are substantially larger than those in the region $E \gg 0.5U$ (see Fig. 3).

Figure 5 shows the dependence of $G(E)$ for a higher electrostatic barrier height: $U = 6$, other parameters as in Fig. 4. A greater value of U results in the shift of the maximum and minimum values of G towards higher energies, values of $G(E)$ become lesser on average (except for the resonance energies); the general characteristic of the spectrum is not changed.

The dependence of the conductivity on energy for wider barrier is plotted in Fig. 6 for the following parameters: $D = 6$, $U = 4$, $\alpha = 0.5$; 1; 2 for $G1$, $G2$, $G3$, respectively. It exhibits the pronounced maxima at the points $E_s = U/(1 + \alpha)$. Also the pattern of lines with the Fabry–Perot resonances is substantially changed in both regions: $E > U$ and $E < E_s$; both the period and the amplitude of the oscillations are substantially reduced in comparison with the

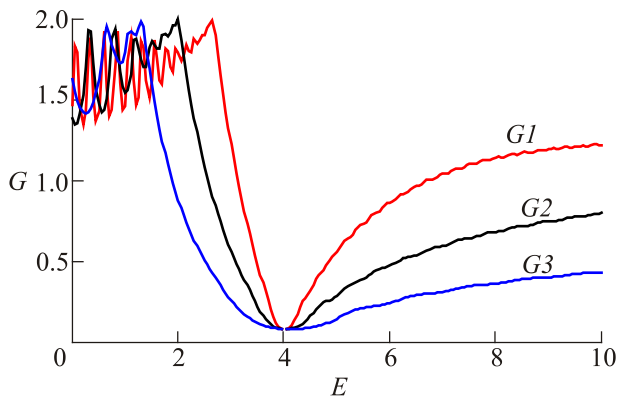


Fig. 6. (Color online) $G(E)$ dependence for wider barrier: $D = 6$; $U = 4$, $\alpha = 0.5$; 1; 2 for $G1$, $G2$, $G3$, respectively.

respective lines in Figs. 4 and 5. Values of $G(E)$ decrease on average with increasing in the width of the barrier (except for the resonance energies).

4. Conclusions

The object of our investigation is a 3D topological insulator the surface states of which are described by the Dirac-like equation. We use the continuum model and the transfer matrix method for our evaluations. The transmission spectra, i.e., the dependences, of the transmission rates on the quasiparticles energy and on the angle of incidence through the Fermi velocity barrier and the electrostatic barrier are calculated. It is shown that these spectra display the resonant tunneling character. The dependence of spectra on the magnitude of the electrostatic potential, as well as on the values of the Fermi velocity in the barrier and in the out-of-barrier regions, is studied.

The most characteristic and interesting property of the investigated structures is the manifestation in them of a phenomenon known as the supertunneling: for some energy values, its quantum transparency is perfect for all angles of incidence of quasiparticles on the barrier. For the case of tunneling through the combined electrostatic and the Fermi velocities barriers the supertunneling takes place for energies not equal to half the electrostatic barrier (as in the case of absence of the velocity barriers), these values being dependent on the Fermi velocity barrier magnitude. An analytical formula for this dependence is deduced. An important feature is also the presence in the transmission spectra of the critical angle of incidence of quasiparticles on the barriers. In a wide range of parameter values, barriers become opaque for particles that fall on them at an angle that exceeds a critical angle. This feature allows to use the investigated structures, in particular, as the wavevector filters. The conductivity of the structure considered exhibits the features associated with the $T(E)$ dependences. The results of our work can be applied for controlling the transmission spectra of the 3D topological insulators.

1. T.O. Wehling, A.M. Black-Schaffer, and A.V. Balatsky, *Adv. Phys.* **63**, 1 (2014).
2. Y. Tanaka, T. Yokohama, and N. Nagaosa, *Phys. Rev.* **103**, 107002 (2009).
3. L. Fu, *Phys. Rev. Lett.* **103**, 266801 (2009).
4. R. Takahashi and S. Murakami, *Phys. Rev.* **107**, 166805 (2011).
5. A. Iurov, G. Gumbs, O. Roslyak, and D. Huang, *J. Phys.: Condens. Matter* **24**, 015303 (2012).
6. A. Iurov, G. Gumbs, O. Roslyak, and D. Huang, *J. Phys.: Condens. Matter* **25**, 135502 (2013).
7. M. Alos-Palop, P. Rakesh, and M. Blaauboer, *Phys. Rev. B* **87**, 035432 (2013).
8. H. Li, J. Shao, H. Zhang, Y. Dao-Xin, and G. Yang, *J. Appl. Phys.* **114**, 093703 (2013).
9. Y. Takagaki, *J. Phys.: Condens. Matter* **28**, 025302 (2016).

10. Diptiman Sen and Oindrila Deb, *Phys. Rev. B* **85**, 245402 (2012).
11. Zhenhua Wu, F.M. Peeters, and Kai Chang, *Phys. Rev. B* **82**, 115211 (2010).
12. Y.J. Zheng, J.T. Song, and Y.-X. Li, *Chin. Phys.* **25**, 037301 (2016).
13. J.-T. Song, Y.-X. Li, and Q.-f. Sun, *J. Phys.: Condens. Matter* **26**, 185007 (2014).
14. L. Liu, Yu-Xian Li, and J. Liu, *Phys. Lett. A* **376**, 3342 (2012).
15. Y. Wang, Y. Liu, and B. Wang, *Physica E* **53**, 186 (2013).
16. L. Sun, C. Fang, and T. Liang, *Chin. Phys. Lett.* **30**, 047201 (2013).
17. A. Raoux, M. Polini, R. Asgari, A.R. Hamilton, R. Fazio, and A.H. MacDonald, *Phys. Rev. B* **81**, 073407 (2010).
18. A. Concha and Z. Tešanović, *Phys. Rev. B* **82**, 033413 (2010).
19. J.H. Yuan, J.J. Zhang, Q.J. Zeng, J.P. Zhang, and Z. Cheng, *Physica B* **406**, 4214 (2011).
20. P.M. Krstajic and P. Vasilopoulos, *J. Phys.: Condens. Matter* **23**, 135302 (2011).
21. A.M. Korol, A.I. Sokolenko, and I.V. Sokolenko, *Fiz. Nizk. Temp.* **44**, 1025 (2018) [*Low Temp. Phys.* **44**, 803 (2018)].

Вплив швидкості Фермі на транспортні властивості 3D топологічних ізоляторів

А.М. Король, Н.В. Медвідь

Досліджується балістичний транспорт квазіелектронів на поверхні 3D топологічних ізоляторів крізь бар'єри різної природи: швидкості Фермі та електростатичні бар'єри. Ці бар'єри вважаються прямокутними та одновимірними. Коефіцієнт трансмісії квазіелектронів T в залежності від їх енергії E та кута падіння θ на структуру, що розглядається (спектри трансмісії), розраховується за допомогою ефективного гамільтоніану. Провідність даної структури G обчислюється із використанням формули Ландауера–Буттікера. Показано, що значення T і G істотно залежать від відношення швидкостей Фермі в бар'єрній та позабар'єрній областях $\alpha = v_{F2}/v_{F1}$. Аналізуються залежності цих величин від електростатичного потенціалу. Показано, зокрема, що в даній структурі проявляється ефект супертунелювання, який істотно залежить від значення α . Наведено формулу, що визначає значення енергій, для яких має місце ефект супертунелювання для різних α . У разі нормального кута падіння частинок проявляється

ефект, аналогічний клейнівському парадоксу. Спектри $T(E, \theta)$ та $G(E)$ є вельми чутливими до співвідношення між α , енергією E , величиною електростатичного потенціалу. Отже, змінюючи параметри даної задачі, можна гнучко варіювати залежності $T(E, \theta)$ та $G(E)$ в широких межах. Одержані результати можуть бути застосовані в наноелектроніці, яка використовує топологічні ізолятори.

Ключові слова: топологічні ізолятори, потенційні бар'єри, швидкість Фермі, спектри пропускання.

Влияние скорости Ферми на транспортные свойства 3D топологических изоляторов

А.Н. Король, Н.В. Медведь

Исследуется баллистический транспорт квазиэлектронов на поверхности 3D топологических изоляторов сквозь барьеры различной природы: скорости Ферми и электростатические барьеры. Эти барьеры считаются прямоугольными и одномерными. Коэффициент трансмиссии квазиэлектронов T в зависимости от их энергии E и угла падения на рассматриваемую структуру θ (спектры трансмиссии) рассчитывается с помощью эффективного гамильтониана. Проводимость данной структуры G вычисляется с использованием формулы Ландауэра–Буттикера. Показано, что значения T и G существенно зависят от отношения скоростей Ферми в барьерной и внебарьерной областях $\alpha = v_{F2}/v_{F1}$. Анализируется зависимость этих величин от электростатического потенциала. Показано, в частности, что в данной структуре проявляется эффект супертунелирования, который существенно зависит от значения α . Приведена формула, определяющая значения энергий, для которых имеет место эффект супертунелирования для различных α . В случае нормального угла падения частиц проявляется эффект, аналогичный клейновскому парадоксу. Спектры $T(E, \theta)$ и $G(E)$ весьма чувствительны к соотношению между α , энергией E , величиной электростатического потенциала. Следовательно, изменяя параметры данной задачи, можно гибко варьировать зависимости $T(E, \theta)$ и $G(E)$ в широких пределах. Полученные результаты могут быть применены в нанoeлектронике, которая использует топологические изоляторы.

Ключевые слова: топологические изоляторы, потенциальные барьеры, скорость Ферми, спектры пропускания.